

# 第21章 Relativistic Radiative Transfer

## Plane-Parallel

### Fixed Frame

variables  $IEFP$  in physics

After Fukue, J. 2008, PASJ, 60, 137

After Fukue, J. 2008, PASJ, 60, 627

## 21.1 Relativistic Radiative Transfer Equation and Moment Equations

Let us suppose a plane-parallel moving atmosphere, e.g., a luminous flat disk wind. The radiation energy is transported in the vertical direction, and the gas, itself, also moves in the vertical direction as a *plane-parallel outflow* due to the action of radiation pressure. For simplicity, in the present paper, the radiation field is considered to be sufficiently intense that both the gravitational field of, e.g., the central object and the gas pressure can be ignored. We also assume the gray approximation, where the opacities do not depend on the frequency. As for the order of the flow velocity  $v$ , we consider the fully special relativistic regime.

The radiative transfer equations are given in several literatures (Chandrasekhar 1960; Mihalas 1970; Rybicki, Lightman 1979; Mihalas, Mihalas 1984; Shu 1991; Kato et al. 1998, 2008; Mihalas, Auer 2001; Peraiah 2002; Castor 2004). The basic equations for relativistic radiation hydrodynamics are given in, e.g., the appendix E of Kato et al. (2008) in general and vertical forms, where the quantities are expressed in the inertial frame. The relativistic radiation hydrodynamic equations in the laboratory frame are also derived and discussed in the seminal paper by Mihalas and Auer (2001) in some details.

In a general form the radiative transfer equation in the inertial (fixed) frame is expressed as

$$\begin{aligned} \frac{1}{c} \frac{\partial I}{\partial t} + (\mathbf{l} \cdot \nabla) I &= \rho \gamma^{-3} \left(1 - \frac{\mathbf{v} \cdot \mathbf{l}}{c}\right)^{-3} \left[ \frac{j_0}{4\pi} - (\kappa_0^{\text{abs}} + \kappa_0^{\text{sca}}) \gamma^4 \left(1 - \frac{\mathbf{v} \cdot \mathbf{l}}{c}\right)^4 I \right. \\ &\quad \left. + \frac{\kappa_0^{\text{sca}}}{4\pi} \frac{3}{4} \gamma^{-2} \left(1 - \frac{\mathbf{v} \cdot \mathbf{l}}{c}\right)^{-2} \left\{ \gamma^4 \left[ \left(1 - \frac{\mathbf{v} \cdot \mathbf{l}}{c}\right)^2 + \left(\frac{v^2}{c^2} - \frac{\mathbf{v} \cdot \mathbf{l}}{c}\right)^2 \right] cE \right. \right. \\ &\quad \left. \left. + 2\gamma^2 \left(\frac{v^2}{c^2} - \frac{\mathbf{v} \cdot \mathbf{l}}{c}\right) \mathbf{F} \cdot \mathbf{l} - 2\gamma^4 \left[ \left(1 - \frac{\mathbf{v} \cdot \mathbf{l}}{c}\right)^2 + \left(1 - \frac{\mathbf{v} \cdot \mathbf{l}}{c}\right) \left(\frac{v^2}{c^2} - \frac{\mathbf{v} \cdot \mathbf{l}}{c}\right) \right] \frac{\mathbf{v} \cdot \mathbf{F}}{c} \right\} \right] \end{aligned}$$

$$+l_i l_j c P^{ij} - 2\gamma^2 \left(1 - \frac{\mathbf{v} \cdot \mathbf{l}}{c}\right) v_i l_j P^{ij} + 2\gamma^4 \left(1 - \frac{\mathbf{v} \cdot \mathbf{l}}{c}\right)^2 \frac{v_i v_j P^{ij}}{c} \Bigg], \quad (21.1)$$

Here,  $\mathbf{v}$  is the flow velocity,  $c$  is the speed of light, and  $\gamma (= 1/\sqrt{1-v^2/c^2})$  is the Lorentz factor. In the left-hand side the frequency-integrated specific intensity  $I$  and the direction cosine  $\mathbf{l}$  are quantities measured in the inertial (fixed) frame. In the right-hand side, the mass density  $\rho$ , the frequency-integrated mass emissivity  $j_0$ , the frequency-integrated mass absorption coefficient  $\kappa_0^{\text{abs}}$ , and the frequency-integrated mass scattering coefficient  $\kappa_0^{\text{sca}}$  are quantities measured in the comoving (fluid) frame, whereas the frequency-integrated radiation energy density  $E$ , the frequency-integrated radiative flux  $\mathbf{F}$ , and the frequency-integrated radiation stress tensor  $P^{ij}$  are quantities measured in the inertial (fixed) frame.

In the plane-parallel geometry with the vertical axis  $z$  and the direction cosine  $\mu (= \cos \theta)$ , the transfer equation is expressed as

$$\begin{aligned} \mu \frac{dI}{dz} = & \rho \frac{1}{\gamma^3 (1 - \beta\mu)^3} \left[ \frac{j_0}{4\pi} - (\kappa_0^{\text{abs}} + \kappa_0^{\text{sca}}) \gamma^4 (1 - \beta\mu)^4 I + \frac{\kappa_0^{\text{sca}}}{4\pi} \frac{3}{4} \gamma^2 \left\{ \left[ 1 + \frac{(\mu - \beta)^2}{(1 - \beta\mu)^2} \beta^2 + \frac{(1 - \beta^2)^2}{(1 - \beta\mu)^2} \frac{1 - \mu^2}{2} \right] cE \right. \right. \\ & \left. \left. - \left[ 1 + \frac{(\mu - \beta)^2}{(1 - \beta\mu)^2} \right] 2F\beta + \left[ \beta^2 + \frac{(\mu - \beta)^2}{(1 - \beta\mu)^2} - \frac{(1 - \beta^2)^2}{(1 - \beta\mu)^2} \frac{1 - \mu^2}{2} \right] cP \right\} \right], \end{aligned} \quad (21.2)$$

where  $\beta (= v/c)$  is the normalized vertical speed, and  $F$  and  $P$  are the vertical component of the radiative flux and the radiation stress tensor measured in the inertial frame, respectively.

For matter, the continuity equation, the equation of motion, and the energy equation become, respectively,

$$\rho c u = \rho \gamma \beta c = J \quad (= \text{const.}), \quad (21.3)$$

$$c^2 u \frac{du}{dz} = c^2 \gamma^4 \beta \frac{d\beta}{dz} = -\frac{d\psi}{dz} - \gamma^2 \frac{c^2}{\varepsilon + p} \frac{dp}{dz} + \frac{\rho c^2}{\varepsilon + p} \frac{\kappa_0^{\text{abs}} + \kappa_0^{\text{sca}}}{c} \gamma^3 \left[ F(1 + \beta^2) - (cE + cP)\beta \right], \quad (21.4)$$

$$0 = \frac{q^+}{\rho} - \left( j_0 - \kappa_0^{\text{abs}} cE \gamma^2 - \kappa_0^{\text{abs}} cP u^2 + 2\kappa_0^{\text{abs}} F \gamma u \right), \quad (21.5)$$

where  $u (= \gamma\beta)$  is the vertical four velocity,  $J$  the mass-loss rate per unit area,  $\psi$  the gravitational potential,  $\varepsilon$  the internal energy per unit proper volume,  $p$  the gas pressure, and  $q^+$  the internal heating. In the energy equation (9.5) the advection terms in the left-hand side are dropped under the present cold approximation (radiative equilibrium). We do not use the equation of motion since we will assume that the flow speed is constant.

For radiation, the zeroth and first moment equations, and the closure relation become, respectively,

$$\frac{dF}{dz} = \rho \gamma \left[ j_0 - \kappa_0^{\text{abs}} cE + \kappa_0^{\text{sca}} (cE + cP) \gamma^2 \beta^2 + \kappa_0^{\text{abs}} F \beta - \kappa_0^{\text{sca}} F (1 + \beta^2) \gamma^2 \beta \right], \quad (21.6)$$

$$\frac{dP}{dz} = \frac{\rho \gamma}{c} \left[ j_0 \beta - \kappa_0^{\text{abs}} F + \kappa_0^{\text{abs}} cP \beta - \kappa_0^{\text{sca}} F \gamma^2 (1 + \beta^2) + \kappa_0^{\text{sca}} (cE + cP) \gamma^2 \beta \right], \quad (21.7)$$

$$cP(1 - f\beta^2) = cE(f - \beta^2) + 2F\beta(1 - f), \quad (21.8)$$

where  $f(\tau, \beta)$  is the variable Eddington factor, which is defined by  $f = P_{\text{co}}/E_{\text{co}}$ ,  $E_{\text{co}}$  and  $P_{\text{co}}$  being the comoving quantities, and generally depends on the velocity and its gradient as well as the optical depth (Fukue 2006b, 2008b). In the present approximation, however,  $f$  is automatically determined to be 1/3 as will be shown later.

Eliminating  $j_0$  using the energy equation (9.5), the transfer equation (9.2) becomes

$$\begin{aligned} \mu \frac{dI}{dz} = & \rho \frac{1}{\gamma^3(1-\beta\mu)^3} \left[ -(\kappa_0^{\text{abs}} + \kappa_0^{\text{sca}}) \gamma^4 (1-\beta\mu)^4 I + \frac{q^+}{4\pi\rho} + \frac{\kappa_0^{\text{abs}}}{4\pi} \gamma^2 (cE - 2F\beta + \beta^2 cP) \right. \\ & + \frac{\kappa_0^{\text{sca}}}{4\pi} \frac{3}{4} \gamma^2 \left\{ \left[ 1 + \frac{(\mu-\beta)^2}{(1-\beta\mu)^2} \beta^2 + \frac{(1-\beta^2)^2}{(1-\beta\mu)^2} \frac{1-\mu^2}{2} \right] cE \right. \\ & \left. \left. - \left[ 1 + \frac{(\mu-\beta)^2}{(1-\beta\mu)^2} \right] 2F\beta + \left[ \beta^2 + \frac{(\mu-\beta)^2}{(1-\beta\mu)^2} - \frac{(1-\beta^2)^2}{(1-\beta\mu)^2} \frac{1-\mu^2}{2} \right] cP \right\} \right]. \end{aligned} \quad (21.9)$$

Introducing the optical depth defined by

$$d\tau = -(\kappa_0^{\text{abs}} + \kappa_0^{\text{sca}}) \rho dz, \quad (21.10)$$

the transfer equation (9.9) finally becomes

$$\begin{aligned} \mu \frac{dI}{d\tau} = & \frac{1}{\gamma^3(1-\beta\mu)^3} \left[ \gamma^4 (1-\beta\mu)^4 I - \frac{1}{4\pi} \frac{\kappa_0^{\text{abs}}}{\kappa_0^{\text{abs}} + \kappa_0^{\text{sca}}} \gamma^2 (cE - 2F\beta + \beta^2 cP) \right. \\ & - \frac{1}{4\pi} \frac{\kappa_0^{\text{sca}}}{\kappa_0^{\text{abs}} + \kappa_0^{\text{sca}}} \frac{3}{4} \gamma^2 \left\{ \left[ 1 + \frac{(\mu-\beta)^2}{(1-\beta\mu)^2} \beta^2 + \frac{(1-\beta^2)^2}{(1-\beta\mu)^2} \frac{1-\mu^2}{2} \right] cE \right. \\ & \left. - \left[ 1 + \frac{(\mu-\beta)^2}{(1-\beta\mu)^2} \right] 2F\beta + \left[ \beta^2 + \frac{(\mu-\beta)^2}{(1-\beta\mu)^2} - \frac{(1-\beta^2)^2}{(1-\beta\mu)^2} \frac{1-\mu^2}{2} \right] cP \right\} \left. \right] \\ = & \gamma(1-\beta\mu) I - \frac{1-A}{4\pi} \frac{1}{\gamma(1-\beta\mu)^3} (cE - 2F\beta + \beta^2 cP) \\ & - \frac{A}{4\pi} \frac{3}{4} \frac{1}{\gamma(1-\beta\mu)^3} \left\{ \left[ 1 + \frac{(\mu-\beta)^2}{(1-\beta\mu)^2} \beta^2 + \frac{(1-\beta^2)^2}{(1-\beta\mu)^2} \frac{1-\mu^2}{2} \right] cE \right. \\ & \left. - \left[ 1 + \frac{(\mu-\beta)^2}{(1-\beta\mu)^2} \right] 2F\beta + \left[ \beta^2 + \frac{(\mu-\beta)^2}{(1-\beta\mu)^2} - \frac{(1-\beta^2)^2}{(1-\beta\mu)^2} \frac{1-\mu^2}{2} \right] cP \right\}, \end{aligned} \quad (21.11)$$

where

$$A \equiv \frac{\kappa_0^{\text{sca}}}{\kappa_0^{\text{abs}} + \kappa_0^{\text{sca}}} \quad (21.12)$$

is the scattering albedo, and the internal heating  $q^+$  is dropped.

Similarly, moment equations (9.6) and (9.7), with the help of continuity equation (9.3) and the closure relation (9.8), become (cf. Fukue 2005b, 2006b)

$$\frac{dF}{d\tau} = \gamma^3 \beta [F(1+\beta^2) - (cE + cP)\beta] = \gamma \beta \frac{F(f+\beta^2) - cP(1+f)\beta}{f-\beta^2}, \quad (21.13)$$

$$c \frac{dP}{d\tau} = \gamma^3 [F(1+\beta^2) - (cE + cP)\beta] = \gamma \frac{F(f+\beta^2) - cP(1+f)\beta}{f-\beta^2}. \quad (21.14)$$

Here, we dropped the gravitational and pressure forces as well as the internal heating.

## 21.2 Solutions of Moment Equations

In the present paper we assume that the flow speed is constant, but the source function is not, and seek the analytical solutions of moment equations (9.13) and (9.14). We also assume that the Eddington factor does not depend on the optical depth.

### 21.2.1 General Solutions

If equation (9.13) is divided by equation (9.14), we have

$$\frac{dF}{cdP} = \beta, \quad (21.15)$$

which is integrated to give

$$F = \beta cP + F_1(\beta), \quad (21.16)$$

where  $F_1(\beta)$  is an arbitrary function of  $\beta$ .

Inserting this relation (9.16) into equations (9.13) and (9.14), we can easily integrate equations (9.13) and (9.14) to give the following forms:

$$F = \gamma^2(1+f)F_1(\beta) - C_F(\beta)e^{-\frac{\beta}{\gamma(f-\beta^2)}\tau}, \quad (21.17)$$

$$cP = \frac{\gamma^2(f+\beta^2)}{\beta}F_1(\beta) - C_P(\beta)e^{-\frac{\beta}{\gamma(f-\beta^2)}\tau}, \quad (21.18)$$

where  $C_F(\beta)$  and  $C_P(\beta)$  are arbitrary functions of  $\beta$ .

In order to both solutions (9.17) and (9.18) are consistent with each other,  $C_F = C_P\beta$  and we have

$$cP = \frac{1}{\beta} \left[ \gamma^2(f+\beta^2)F_1(\beta) - C_F(\beta)e^{-\frac{\beta}{\gamma(f-\beta^2)}\tau} \right], \quad (21.19)$$

and furthermore, from the closure relation (9.8), we also have

$$cE = \frac{1}{\beta(f-\beta^2)} \left[ (f-\beta^2)(1+f\beta^2)\gamma^2 F_1(\beta) - (1-2\beta+f\beta^2)C_F(\beta)e^{-\frac{\beta}{\gamma(f-\beta^2)}\tau} \right]. \quad (21.20)$$

With the help of arbitrariness in  $C_F$ , we can express general solutions (9.17), (9.19), and (9.20) as

$$cE = \frac{\gamma^2 F_1}{\beta} \left[ (1+f\beta^2) - (1-2\beta+f\beta^2)C_1(\beta)e^{-\frac{\beta}{\gamma(f-\beta^2)}\tau} \right] \quad (21.21)$$

$$F = \gamma^2 F_1 \left[ (1+f) - (f-\beta^2)C_1(\beta)e^{-\frac{\beta}{\gamma(f-\beta^2)}\tau} \right], \quad (21.22)$$

$$cP = \frac{\gamma^2 F_1}{\beta} \left[ (f+\beta^2) - (f-\beta^2)C_1(\beta)e^{-\frac{\beta}{\gamma(f-\beta^2)}\tau} \right], \quad (21.23)$$

where  $C_1(\beta) = \gamma^2(f-\beta^2)F_1C_F$  is an arbitrary function of  $\beta$ .

These equations (9.21)–(9.23) are general solutions of relativistic moment equations for plane-parallel vertical flows at a constant speed. In the limit of  $\beta \rightarrow 0$ , these solutions approach the Milne-Eddington ones, as long as  $1 - C_F \sim \beta$  for small  $\beta$ .

### 21.2.2 Special Solutions

Next, we derive more special solutions under the appropriate boundary conditions. For the present plane-parallel flow at a constant flow speed, the boundary conditions should be imposed at the flow top, where the optical depth is zero.

At the flow top of a moving photosphere at a relativistic speed, the usual boundary conditions for a static atmosphere is inadequate, as already pointed out in Fukue (2005b). Namely, the radiation field just above the flow top changes when the gas itself does move upward, since the direction and intensity of radiation change due to the relativistic aberration and Doppler effect (cf. Kato et al. 1998, 2008; Fukue 2000). If a flat infinite plane with surface intensity  $I_s$  in the comoving frame is not static, but moving upward at a speed  $v_s$  ( $= c\beta_s$ , and the corresponding Lorentz factor is  $\gamma_s$ ), where the subscript  $s$  denotes the values at the surface, then, just above the surface, the radiation energy density  $E_s$ , the radiative flux  $F_s$ , and the radiation pressure  $P_s$  measured

in the inertial frame become, respectively,

$$cE_s = 2\pi I_s \gamma_s^2 \frac{3 + 3\beta_s + \beta_s^2}{3}, \quad (21.24)$$

$$F_s = 2\pi I_s \gamma_s^2 \frac{3 + 8\beta_s + 3\beta_s^2}{6}, \quad (21.25)$$

$$cP_s = 2\pi I_s \gamma_s^2 \frac{1 + 3\beta_s + 3\beta_s^2}{3}. \quad (21.26)$$

It should be noted that these boundary conditions imply that the Eddington factor  $f$  defined in the comoving frame is  $1/3$ .

Using these boundary conditions (9.24)–(9.26) to general solutions (9.21)–(9.23), we can determine the arbitrary functions  $F_1$  and  $C_1$  as

$$F_1 = \pi I_s (1 + 2\beta), \quad (21.27)$$

$$C_1 = \frac{1}{1 + 2\beta}, \quad (21.28)$$

and the Eddington factor  $f$  is automatically fixed as  $1/3$ .

Finally, the solutions of moment equations for relativistic plane-parallel flows at a constant speed are explicitly written as

$$\frac{cE}{\pi I_s} = \frac{\gamma^2}{\beta} \left[ (1 + f\beta^2)(1 + 2\beta) - (1 - 2\beta + f\beta^2)e^{-\frac{\beta}{\gamma(f - \beta^2)}\tau} \right] \quad (21.29)$$

$$\frac{F}{\pi I_s} = \gamma^2 \left[ (1 + f)(1 + 2\beta) - (f - \beta^2)e^{-\frac{\beta}{\gamma(f - \beta^2)}\tau} \right], \quad (21.30)$$

$$\frac{cP}{\pi I_s} = \frac{\gamma^2}{\beta} \left[ (f + \beta^2)(1 + 2\beta) - (f - \beta^2)e^{-\frac{\beta}{\gamma(f - \beta^2)}\tau} \right], \quad (21.31)$$

where  $f = 1/3$ .

In the limit of small  $\beta$ , these solutions approach

$$\frac{cE}{\pi I_s} \sim 2 + \frac{1}{f}\tau, \quad (21.32)$$

$$\frac{F}{\pi I_s} \sim 1 + 2(1 + f)\beta + \beta\tau, \quad (21.33)$$

$$\frac{cP}{\pi I_s} \sim 2f + \tau, \quad (21.34)$$

which are just the Milne-Eddington solutions for a static plane-parallel atmosphere. Hence, the present solutions (9.29)–(9.31) are the Milne-Eddington ones extended to the case for the relativistic plane-parallel flow.

By the Lorentz transformation, it is easy to obtain the solutions in the comoving frame. Namely, the solutions of moment equations in the comoving frame are explicitly written as

$$\frac{cE_{co}}{\pi I_s} = \frac{1}{\pi I_s} \gamma^2 (cE - 2\beta F + \beta^2 cP) = \frac{1}{\beta} \left[ (1 + 2\beta) - e^{-\frac{\beta}{\gamma(f - \beta^2)}\tau} \right] \quad (21.35)$$

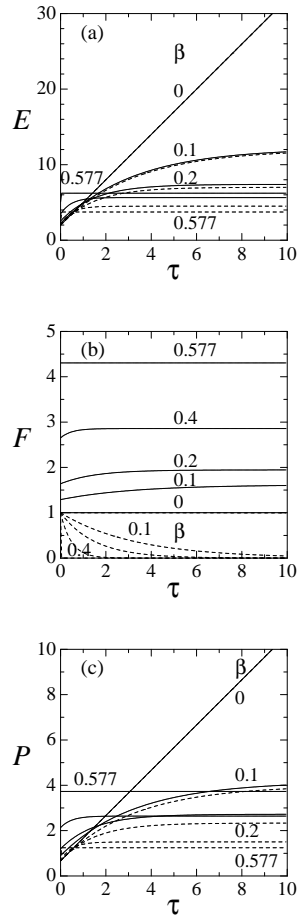
$$\frac{F_{co}}{\pi I_s} = \frac{1}{\pi I_s} \gamma^2 [(1 + \beta^2)F - \beta(cE + cP)] = e^{-\frac{\beta}{\gamma(f - \beta^2)}\tau}, \quad (21.36)$$

$$\frac{cP_{co}}{\pi I_s} = \frac{1}{\pi I_s} \gamma^2 (\beta^2 cE - 2\beta F + cP) = \frac{f}{\beta} \left[ (1 + 2\beta) - e^{-\frac{\beta}{\gamma(f - \beta^2)}\tau} \right] \quad (21.37)$$

where  $f = 1/3$ . Hence, as already stated, in the comoving frame  $P_{co}/E_{co} = f = 1/3$ , exactly.

In figure 1, Milne-Eddington solutions of moment equations for relativistic plane-parallel flows are shown as a function of the optical depth  $\tau$ : (a) Radiation energy density  $E$ , (b) radiative flux  $F$ , and (c) radiation pressure  $P$ , where the radiation quantities are normalized by  $\pi I_s$ . The solid curves represent the quantities in the inertial frame, whereas the dashed ones mean those in the comoving frame. The flow speed  $\beta$  are set to be 0, 0.1, 0.2, 0.4, and 0.577.

In figure 1a, the radiation energy density  $E$  normalized by  $\pi I_s/c$  is plotted for various  $\beta$ . As was already stated, and as is easily seen in figure 1a, when the flow speed is small, the solution reduces to the usual Milne-Eddington one for a static plane-parallel atmosphere;  $cE/(\pi I_s) \sim 2 + 3\tau$ . As the flow speed increases, the radiation energy density becomes constant. This means that the radiation energy itself is advected along with the flow, and it is constant without the internal heating. Furthermore, comparing the radiation energy density in the inertial frame (solid curves) and those in the comoving frame (dashed ones), the radiation energy density in the inertial frame is enhanced due to the relativistic motion.



☒ 21.1: Milne-Eddington solutions for relativistic plane-parallel flows: (a) Normalized radiation energy density, (b) normalized radiative flux, and (c) normalized radiation pressure. The solid curves represent the quantities in the inertial frame, whereas the dashed ones mean those in the comoving frame. The values of  $\beta$  are 0, 0.1, 0.2, 0.4, and 0.577.

In figure 1b, the radiative flux  $F$  normalized by  $\pi I_s$  is plotted for various  $\beta$ . When the flow speed is small, the solution reduces to the usual Milne-Eddington one for a static plane-parallel atmosphere;  $F/(\pi I_s) \sim 1$ . As the flow speed increases, the radiative flux in the inertial frame (solid curves) is enhanced more and more due to the relativistic effect. The radiative flux in the comoving frame (dashed ones), on the other hand, reduces exponentially. This means that in the relativistically moving plane-parallel flows without the internal heating the radiative flux in the comoving frame vanishes since the radiation energy (and pressure) is advected with the flow and there is no gradient in the radiation pressure.

In figure 1c, the radiation pressure  $P$  normalized by  $\pi I_s/c$  is plotted for various  $\beta$ . When the flow speed is small, the solution reduces to the usual Milne-Eddington one for a static plane-parallel atmosphere;  $cP/(\pi I_s) \sim 2/3 + \tau$ . As the flow speed increases, the radiation pressure becomes constant. Furthermore, comparing the radiation energy pressure in the inertial frame (solid curves) and those in the comoving frame (dashed ones), the radiation pressure in the inertial frame is enhanced due to the relativistic motion.

It should be noted that in the present solution the Eddington factor  $f$  is set to be  $1/3$ , and therefore, the flow speed  $\beta$  is restricted within  $\beta < 1/\sqrt{3} \sim 0.5774$  (cf. Fukue 2005a).

### 21.3 Solutions of Transfer Equation

Since we obtain the analytical forms of radiation moments, and we assume that the flow speed is constant, we can analytically integrate the relativistic radiation transfer equation (9.11).

By inserting the solutions (9.29)–(9.31) into the transfer equation (9.11), and setting  $f = 1/3$ , the transfer equation (9.11) is rewritten as

$$\mu \frac{dI}{d\tau} = \gamma(1 - \beta\mu)I - \frac{\pi I_s}{4\pi} \frac{1}{\gamma^3(1 - \beta\mu)^3} \frac{1}{\beta} \left[ (1 + 2\beta) - e^{-\frac{\beta}{\gamma(f - \beta^2)}\tau} \right] \quad (38)$$

where  $f = 1/3$ .

It is straightforward to integrate this equation (9.38) (cf. Fukue, Akizuki 2006b; Fukue 2007). After several partial integrations, we obtain both an outward intensity  $I(\tau, \mu, \beta)$  ( $\mu > 0$ ),

$$\begin{aligned}
I(\tau, \mu, \beta) &= \frac{\pi I_s}{4\pi} \frac{1}{\gamma^4(1-\beta\mu)^4} \frac{1}{\beta} \left[ (1+2\beta) - \frac{1}{1 + \frac{\beta\mu}{\gamma^2(1-\beta\mu)(f-\beta^2)}} e^{-\frac{\beta}{\gamma(f-\beta^2)}\tau} \right] \\
&\quad - \frac{\pi I_s}{4\pi} \frac{1}{\gamma^4(1-\beta\mu)^4} \frac{1}{\beta} \left[ (1+2\beta) - \frac{1}{1 + \frac{\beta\mu}{\gamma^2(1-\beta\mu)(f-\beta^2)}} e^{-\frac{\beta}{\gamma(f-\beta^2)}\tau_0} \right] \\
&\quad + I(\tau_0, \mu) e^{\frac{\gamma(1-\beta\mu)}{\mu}(\tau-\tau_0)} \\
&\sim \frac{\pi I_s}{4\pi} \frac{1}{\gamma^4(1-\beta\mu)^4} \frac{1}{\beta} \left[ (1+2\beta) - \frac{1}{1 + \frac{\beta\mu}{\gamma^2(1-\beta\mu)(f-\beta^2)}} e^{-\frac{\beta}{\gamma(f-\beta^2)}\tau} \right]
\end{aligned}$$

and an inward intensity  $I(\tau, \mu, \beta)$  ( $\mu < 0$ ),

$$\begin{aligned}
I(\tau, \mu, \beta) &= \frac{\pi I_s}{4\pi} \frac{1}{\gamma^4(1-\beta\mu)^4} \frac{1}{\beta} \left[ (1+2\beta) - \frac{1}{1 + \frac{\beta\mu}{\gamma^2(1-\beta\mu)(f-\beta^2)}} e^{-\frac{\beta}{\gamma(f-\beta^2)}\tau} \right] \\
&\quad - \frac{\pi I_s}{4\pi} \frac{1}{\gamma^4(1-\beta\mu)^4} \frac{1}{\beta} \left[ (1+2\beta) - \frac{1}{1 + \frac{\beta\mu}{\gamma^2(1-\beta\mu)(f-\beta^2)}} e^{-\frac{\beta}{\gamma(f-\beta^2)}\tau_0} \right] \\
&\quad + I(\tau_0, \mu) e^{\frac{\gamma(1-\beta\mu)}{\mu}(\tau-\tau_0)}
\end{aligned}$$

where  $I(\tau_0, \mu)$  is the boundary value at the flow base of the optical depth  $\tau_0$ .

In the limit of small  $\beta$ , this solution reduces to the usual Milne-Eddington one; e.g., for  $\mu > 0$

$$I(\tau, \mu, 0) \sim \frac{\pi I_s}{4\pi} \left[ (2+3\tau+3\mu) - (2+3\tau_0+3\mu)e^{\frac{\tau-\tau_0}{\mu}} \right] + I(\tau_0, \mu) e^{\frac{\tau-\tau_0}{\mu}}. \quad (21.41)$$

Finally, the emergent intensity  $I(0, \mu, \beta)$  ( $\mu > 0$ ) at the flow surface of  $\tau = 0$

becomes

$$\begin{aligned}
I(0, \mu, \beta) &= \frac{\pi I_s}{4\pi} \frac{1}{\gamma^4(1-\beta\mu)^4} \frac{2 + \frac{(1+2\beta)\mu}{\gamma^2(1-\beta\mu)(f-\beta^2)}}{1 + \frac{\beta\mu}{\gamma^2(1-\beta\mu)(f-\beta^2)}} \\
&\quad - \frac{\pi I_s}{4\pi} \frac{1}{\gamma^4(1-\beta\mu)^4} \frac{1}{\beta} \left[ (1+2\beta) - \frac{1}{1 + \frac{\beta\mu}{\gamma^2(1-\beta\mu)(f-\beta^2)}} e^{-\frac{\beta}{\gamma(f-\beta^2)}\tau_0} \right] \\
&\quad + I(\tau_0, \mu) e^{-\frac{\gamma(1-\beta\mu)}{\mu}\tau_0} \\
&\sim \frac{\pi I_s}{4\pi} \frac{1}{\gamma^4(1-\beta\mu)^4} \frac{2 + \frac{(1+2\beta)\mu}{\gamma^2(1-\beta\mu)(f-\beta^2)}}{1 + \frac{\beta\mu}{\gamma^2(1-\beta\mu)(f-\beta^2)}} \quad \text{for large } \tau_0.
\end{aligned}$$

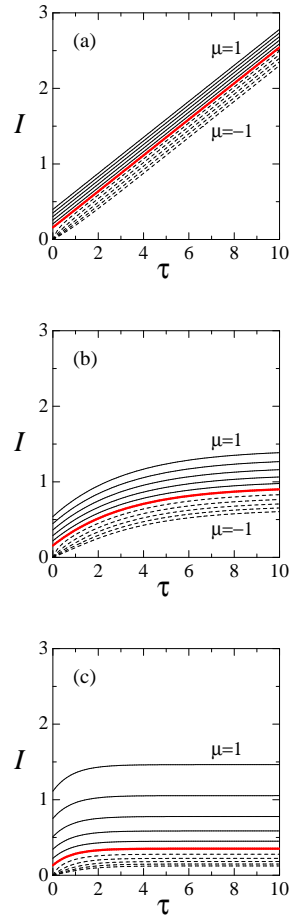
for large  $\tau_0$  (21.39)

In figure 2, the specific intensity normalized by  $I_s$  of Milne-Eddington solutions of transfer equation for relativistic plane-parallel flows are shown as a function of the optical depth  $\tau$  for several values of  $\mu$  and  $\beta$ . The values of  $\beta$  are (a) 0, (b) 0.1, and (c) 0.3. In each figure, the thick solid curves are for  $\mu = 0$ , the solid curves are for  $\mu = 0.2, 0.4, 0.6, 0.8$ , and 1 from bottom to top, while the dashed ones are for  $\mu = -0.2, -0.4, -0.6, -0.8$ , and  $-1$  from top to bottom.

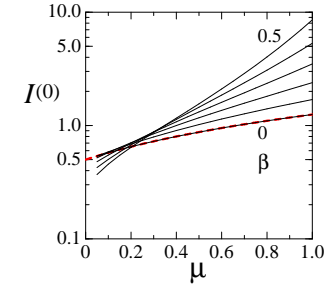
As is seen in figure 2, in the case of small  $\beta$  (figure 2a), the usual Milne-Eddington solution for a static plane-parallel atmosphere is well reproduced. As the flow speed increases, the specific intensity becomes constant, and is enhanced ( $\mu > 0$ ) or diminished ( $\mu < 0$ ) due to the relativistic vertical motion.

In figure 3, the emergent intensity  $I(0, \mu, \beta)$  normalized by  $I_s$  of Milne-Eddington solutions of transfer equation for relativistic plane-parallel flows is plotted as a function of  $\mu$  for several values of  $\beta$ . The values of  $\beta$  are 0, 0.1, 0.2, 0.3, 0.4, and 0.5. The dashed line is for the usual Milne-Eddington solution for the static plane-parallel case.

In the limit of  $\beta = 0$ , the present emergent intensity again reduces to the usual Milne-Eddington solution for a static atmosphere. As the flow speed increases, the *relativistic peaking effect* becomes prominent; that is to say, the



⊠ 21.2: Normalized specific intensity of Milne-Eddington solutions for relativistic plane-parallel flows as a function of the optical depth  $\tau$  for several values of  $\mu$  and  $\beta$ . The values of  $\beta$  are (a) 0, (b) 0.1, and (c) 0.3. The values of  $\mu$  are 0 (thick solid curves), 0.2, 0.4, 0.6, 0.8, and 1 (solid curves), and  $-0.2, -0.4, -0.6, -0.8,$  and  $-1$  (dashed ones).



⊠ 21.3: Normalized emergent intensity of Milne-Eddington solutions for relativistic plane-parallel flows as a function of  $\mu$  for several values of  $\beta$ . The values of  $\beta$  are 0, 0.1, 0.2, 0.3, 0.4, and 0.5. The dashed line is for the usual Milne-Eddington solution for the static plane-parallel case.

emergent intensity is strongly enhanced toward the poleward direction, while it is less enhanced in the edgeward direction.